Alternative Splicing of Rice *WRKY62* and *WRKY76* Transcription Factor Genes in Pathogen Defense[1][OPEN]

Jiqin Liu[2], Xujun Chen[2], Xiaoxing Liang, Xiangui Zhou, Fang Yang, Jia Liu, Sheng Yang He, and Zejian Guo*

Key Laboratory of Plant Pathology, MOA, China Agricultural University, Beijing 100193, China (Jiq.L., X.C., X.L., X.Z., F.Y., Jia.L., Z.G.); and Howard Hughes Medical Institute, Department of Energy Plant Research Laboratory, Michigan State University, East Lansing, Michigan 48824 (S.Y.H.)

ORCID IDs: 0000-0002-2697-1919 (Jiq.L.); 0000-0003-4253-1662 (X.L.); 0000-0001-7648-9816 (Jia.L.); 0000-0003-1308-498X (S.Y.H.); 0000-0001-7210-2370 (Z.G.).

The WRKY family of transcription factors (TFs) functions as transcriptional activators or repressors in various signaling pathways. In this study, we discovered that *OsWRKY62* and *OsWRKY76*, two genes of the WRKY IIa subfamily, undergo constitutive and inducible alternative splicing. The full-length OsWRKY62.1 and OsWRKY76.1 proteins formed homocomplexes and heterocomplexes, and the heterocomplex dominates in the nuclei when analyzed in *Nicotiana benthamiana* leaves. Transgenic overexpression of *OsWRKY62.1* and *OsWRKY76.1* in rice (*Oryza sativa*) enhanced plant susceptibility to the blast fungus *Magnaporthe oryzae* and the leaf blight bacterium *Xanthomonas oryzae* pv *oryzae*, whereas RNA interference and loss-of-function knockout plants exhibited elevated resistance. The dsOW62/76 and knockout lines of *OsWRKY62* and *OsWRKY76* also showed greatly increased expression of defense-related genes and the accumulation of phytoalexins. The ratio of full-length versus truncated transcripts changed in dsOW62/76 plants as well as in response to pathogen infection. The short alternative OsWRKY62.2 and OsWRKY76.2 isoforms could interact with each other and with full-length proteins. OsWRKY62.2 showed a reduced repressor activity in planta, and two sequence determinants required for the repressor activity were identified in the amino terminus of OsWRKY62.1. The amino termini of OsWRKY62 and OsWRKY76 splice variants also showed reduced binding to the canonical W box motif. These results not only enhance our understanding of the DNA-binding property, the repressor sequence motifs, and the negative feedback regulation of the IIa subfamily of WRKYs but also provide evidence for alternative splicing of WRKY TFs during the plant defense response.

Plants have evolved a powerful innate immune system to protect themselves from invading pathogens. Pathogen-associated molecular pattern (PAMP)-triggered immunity (PTI) is thought to be the first layer of plant defense mechanisms (Jones and Dangl, 2006; Zipfel and Robatzek, 2010). Upon perception of PAMP molecules such as fungal chitin and bacterial flagellin, the corresponding pattern recognition receptors at the surface of plant cells activate downstream signaling pathways to provide a basal level of defense. Many successful pathogens have evolved effector proteins to suppress

PTI. As a countermeasure, plants developed effector-triggered immunity, which often involves programmed cell death to contain pathogens (Jones and Dangl, 2006). Both PTI and effector-triggered immunity are associated with global transcriptional reprogramming, in which the WRKY family of transcription factors (TFs) play significant roles in orchestrating the transcriptional activation or repression of suites of plant defense genes (Pandey and Somssich, 2009; Agarwal et al., 2011; Bakshi and Oelmüller, 2014).

As a plant-specific gene family, WRKY TFs contain a zinc finger motif within each conserved DNA-binding domain and bind mostly to the consensus W box (with the core nucleotide sequence of TGAC). W boxes are commonly found in the promoters of defense-associated genes, including the *NPR1* gene, which is a key regulator of the salicylic acid-dependent immune response (Yu et al., 2001; Rushton et al., 2010; Fu and Dong, 2013). Mutations of the W boxes have been shown to compromise the induction of the *NPR1* gene (Yu et al., 2001). On the other hand, the expression of at least eight *WRKY* genes is up-regulated by NPR1, suggesting a positive feedback loop in defense activation (Wang et al., 2006).

WRKY TFs also may be posttranscriptionally activated through several pathways, such as phosphorylation by mitogen-activated protein kinases (MPKs) or via interaction with resistance (R) proteins. For example,

Arabidopsis (*Arabidopsis thaliana*) WRKY33 is phosphorylated by MPK3/MPK6 in response to infection by *Botrytis cinerea* and is required for MPK3/MPK6-induced camalexin biosynthesis (Mao et al., 2011). In *Nicotiana benthamiana*, phosphorylated WRKY8 and its phosphor-mimicking mutants are found to have increased binding to the cognate W box and enhanced transactivation activity, respectively (Ishihama et al., 2011). *Panicle blast1* (*Pb1*) is a panicle blast resistance gene, conferring durable resistance to *Magnaporthe oryzae* (Hayashi et al., 2010). The interaction of Pb1 with WRKY45 in the nucleus is important for blast resistance mediated by Pb1 (Inoue et al., 2013). Like Arabidopsis WRKY33, WRKY45 is phosphorylated by OsMPK4 and OsMPK6 (Ueno et al., 2013). In race-specific barley (*Hordeum vulgare*) resistance to *Blumeria graminis*, the R protein MLA10 relocates to the nucleus and forms a complex with HvWRKY1 or HvWRKY2, which belong to the WRKY IIa subfamily (Shen et al., 2007). Finally, XA21, a rice (*Oryza sativa*) pattern recognition receptor for *Xanthomonas oryzae* pv *oryzae* (Xoo), interacts with several proteins, including OsWRKY62, in the nucleus of rice protoplasts (Park and Ronald, 2012).

Three members of the Arabidopsis WRKY IIa subgroup proteins, AtWRKY18, AtWRKY40, and AtWRKY60, were found to interact physically to regulate plant defense responses. Analysis of single, double, and triple mutants and constitutive expression plants demonstrated that these proteins could function in antagonistic, redundant, and distinct roles in response to the hemibiotrophic bacterial pathogen *Pseudomonas syringae* and the necrotrophic fungal pathogen *B. cinerea* (Xu et al., 2006). Genome-wide analysis revealed that AtWRKY18 and AtWRKY40 negatively modulate the expression of positive regulators of defense against the powdery mildew fungus *Golovinomyces orontii* (Pandey et al., 2010). Recently, HvWRKY1, a transcriptional repressor, was shown to interact with MYB6, which functions as a positive regulator of basal and race-specific disease resistance against the barley powdery mildew pathogen (Chang et al., 2013). The active state of the MLA10 receptor is required to release activated MYB6 from HvWRKY1 and stimulate MYB6 binding to its target cis-elements (Chang et al., 2013). These data suggest that protein-protein interactions play a pivotal role in the complicated regulatory network of WRKY-mediated basal and race-specific disease resistance.

The rice WRKY IIa subgroup is composed of *OsWRKY28*, *OsWRKY62*, *OsWRKY71*, and *OsWRKY76*, and three of these genes have been shown to function negatively in disease resistance against *M. oryzae* and/or *Xoo*, except for *OsWRKY71* (Liu et al., 2007; Chujo et al., 2008, 2013; Peng et al., 2008; Yokotani et al., 2013). The WRKY domains of OsWRKY76 and AtWRKY18 are highly homologous (Wu et al., 2005), suggesting that these two genes may have similar biological roles. In addition, *OsWRKY62* and *OsWRKY76* were proposed to derive from an intrachromosomal duplication and subsequent subfunctionalization (Wu et al., 2005). In this study, we analyzed the potential role of *OsWRKY62* and *OsWRKY76* together by characterizing transgenic plants that are intended for overexpression, underexpression, or loss-of-function knockout of each gene or both genes. Our analysis led to unexpected findings of constitutive and inducible alternative splicing of *OsWRKY62* and *OsWRKY76* in pathogen defense.

RESULTS

Formation of Homocomplexes and Heterocomplexes between Full-Length OsWRKY62.1 and OsWRKY76.1 Proteins

In addition to the conserved WRKY domains, IOsWRKY62.1 and OsWRKY76.1 proteins share potential coiled-coil (CC) domains at the N and C termini (Fig. 1A; Supplemental Fig. S1), which prompted us to investigate possible physical interactions between the two proteins. OsWRKY62.1 and OsWRKY76.1 were fused with either the Gal4 DNA-binding domain (in bait vector pBD) or activation domain (in prey vector pAD), and combinations of bait and prey plasmids were introduced into yeast (*Saccharomyces cerevisiae*) cells. Interaction was observed between BD-OW62.1 and AD-OW62.1, BD-OW76.1 and AD-OW76.1, and AD-OW62.1 and BD-OW76.1, indicated by growth of the yeast on selective medium lacking Leu, Trp, His, and adenine (Fig. 1B). We also noticed that BD-OW62.1 exhibited a weak autoactivation activity, which was abolished by deletion of the N-terminal region that is rich in acidic amino acids (OW62ΔN in Fig. 1B). BD-OW62ΔN was still capable of interacting with AD-OW62.1. We generated two truncated OsWRKY76.1 mutants to examine the interacting regions: OW76ΔN containing the WRKY domain and OW76ΔC containing the predicted CC domain could interact with full-length OsWRKY62.1 and OsWRKY76.1, respectively. These results suggest that OsWRKY76.1 contains multiple interaction regions to form a homocomplex or heterocomplex with OsWRKY62.1.

The interaction between OsWRKY62.1 and OsWRKY76.1 also was analyzed by protein pull-down assays. OsWRKY62.1 and OsWRKY76.1 were fused at their N termini with a 6×His tag and at their C termini with a 3×flag or 3×myc tag. The recombinant His-OW76.1-3myc and His-OW62.1-3flag proteins were pulled down with an anti-c-myc affinity gel. As shown in Figure 1C, OsWRKY62.1 and OsWRKY76.1 also can form complexes under this assay condition.

To validate whether OsWRKY62.1 interacts with OsWRKY76.1 in planta, we employed the method of bimolecular fluorescence complementation (BiFC). OsWRKY62.1 and OsWRKY76.1 were fused with the N- and C-terminal domains of yellow fluorescent protein (YFP) under the control of the cauliflower mosaic virus 35S promoter. The fusion proteins were transiently expressed in *N. benthamiana* leaves via *Agrobacterium tumefaciens*-mediated infiltration. Fluorescence was detected in the nuclei of epidermal cells transformed with 35S:OW76.1-YFP[N] and 35S:OW76.1-YFP[C], suggesting that OsWRKY76.1 fusion proteins could interact with each
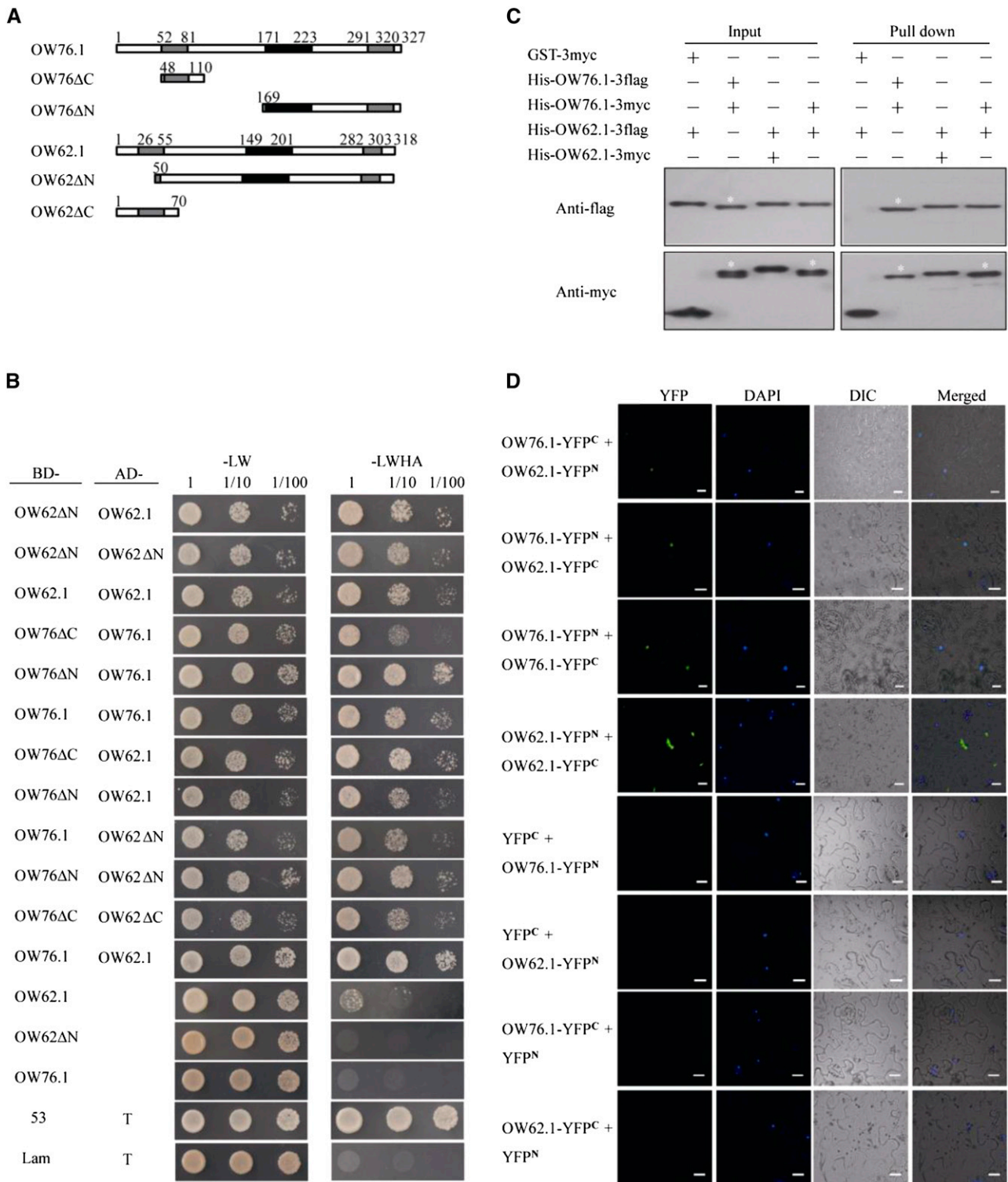
Figure 1. Homocomplex and heterocomplex formation of OsWRKY62.1 and OsWRKY76.1. A, Schematic diagrams of OsWRKY62.1 (OW62.1) and OsWRKY76.1 (OW76.1) proteins. Gray and black boxes represent the predicted CC and WRKY DNA-binding domains, respectively (http://smart.embl-heidelberg.de/smart/show_motifs.pl). The numbers are the amino acid positions in the full-length proteins. B, Analyses of OsWRKY62.1 and OsWRKY76.1 interactions in yeast. OW62.1, OW76.1, and their deletion mutants (OW62ΔN, OW62ΔC, OW76ΔN, and OW76ΔC) were fused to the Gal4 DNA-binding domain (BD) and/ or activation domain (AD). Yeast cells with serial dilutions (1, 1/10, and 1/100) were incubated in synthetic dropout (SD) medium lacking Leu and Trp (-LW; left) or Leu, Trp, His, and adenine (-LWHA; right) and photographed 3 d after plating. Yeast cells

other (Fig. 1D). The nuclear localization of OsWRKY76.1 fusion proteins is consistent with that detected by the expression of 35S:OsWRKY76.1-GFP (Supplemental Fig. S2A). OsWRKY62.1 fusion proteins formed homocomplexes that were detected in unknown structures or aggregates (Fig. 1D). The unique localization of OsWRKY62.1 fusion proteins was confirmed in rice plants stably transformed with 35S:OW62.1-GFP (Supplemental Fig. S2B). Interestingly, fluorescence was detected predominantly in the nuclei of *N. benthamiana* leaves coexpressing OW76.1-YFP^N and OW62.1-YFP^C or OW76.1-YFP^C and OW62.1-YFP^N (Fig. 1D). These results indicate that OsWRKY62.1 and OsWRKY76.1 form heterocomplexes in the nuclei in spite of the unique localization of OsWRKY62.

Expression of *OsWRKY62* and *OsWRKY76* Was Induced by PAMPs, Jasmonate, and Wounding Treatments

Members of the WRKY IIa subgroup have been shown to function in basal and race-specific resistance in barley and Arabidopsis (Xu et al., 2006; Shen et al.., 2007), and *OsWRKY62* and *OsWRKY76* were reported to be induced by *M. oryzae* (Ryu et al., 2006; Shimono et al., 2007). These observations prompted us to examine the expression of *OsWRKY62* and *OsWRKY76* genes in response to PAMPs and other stress signals. We found that both genes showed a pattern of biphasic induction in rice seedlings treated with 10 nM chitin or 0.7 μM flg22, a bioactive 22-amino acid peptide derived from bacterial flagellin (Fig. 2, A and B). The first peak was observed 0.5 h post treatment, and it was followed by the second larger one at 12 h. Overall, the expression patterns of *OsWRKY62* and *OsWRKY76* were similar.

The expression of *OsWRKY62* and *OsWRKY76* genes also was strongly induced after methyl jasmonate (MeJA) treatment or wounding of rice leaves (Fig. 2, C, D, and F). The levels of *OsWRKY62* induction by MeJA were higher compared with those of *OsWRKY76*. The significant up-regulation of a MeJA-responsive marker gene, *OsLOX*, also was observed, indicating the effectiveness of MeJA treatment (Fig. 2E).

To investigate the tissue-specific expression patterns of the two genes, promoters of *OsWRKY62.1* and *OsWRKY76.1* (about 2 kb in length upstream of the translation start site) were fused to the *GUS* gene, and

the resulting constructs were transformed into rice. In Cp-OW76p:GUS T2 transgenic progeny, GUS staining was detected in coleoptiles and roots of 7-d-old seedlings (Fig. 3A) and in lateral roots of 12-d-old plants (Fig. 3B). In contrast, histochemical GUS activity was detected in primary and lateral roots of Cp-OW62p: GUS lines (Fig. 3, A and B). At the reproductive growth stage, *GUS* expression was detected in ligule base, leaf sheath, stem, and stem node, although a higher level was observed in plants harboring the Cp-OW76p:GUS construct (Fig. 3, C and E). At the heading stage, GUS signals were detected in the stamen filaments of Cp-OW76p:GUS plants (Fig. 3D) and in immature seed husks (Fig. 3F), whereas GUS staining was observed strongly in anthers and stigmas of Cp-OW62p:GUS lines (Fig. 3D). In addition, strong GUS activity was found at the cutting sites of Cp-OW76p: GUS plants at higher levels compared with those in Cp-OW62p:GUS plants (Fig. 3C), resembling the expression levels of the two genes induced by wounding (Fig. 2F). Taken together, although *OsWRKY62* and *OsWRKY76* genes exhibited similar expression patterns in response to PAMPs, MeJA, and wounding, the two genes also showed variations in levels of expression and/or in tissue specificity.

OsWRKY62 and *OsWRKY76* Negatively Regulate Resistance against *M. oryzae* and *Xoo*

We generated transgenic rice plants to overexpress or down-regulate *OsWRKY62* and *OsWRKY76* genes, and the resulting transgenic and control plants were inoculated with a virulent strain of the blast fungus *M. oryzae* SZ. As shown in Figure 4, overexpressing lines of *OsWRKY62.1* (OW62.1ox) and *OsWRKY76.1* (OW76.1ox) were more susceptible to the rice blast fungus compared with the wild-type ZH17 control, whereas the RNA interference (RNAi) plants (dsOW62 and dsOW76) showed enhanced resistance against the pathogen. These plants also were inoculated with the *Xoo* strain J18 by the scissor-clipping method. The lesion length was shorter in plants harboring the RNAi constructs and longer in the overexpressing lines compared with the wild-type ZH17 plants (Fig. 4, C and D). These data indicate that *OsWRKY62.1* and *OsWRKY76.1* are negative regulators of disease resistance against *M. oryzae* and *Xoo* in rice.

Figure 1. (*Continued.*)
harboring AD-T with BD-53 or BD-Lam vectors were used as the positive or negative control. C, Pull-down assays of OsWRKY62.1 and OsWRKY76.1 interactions. OW62.1 and OW76.1 were purified with their N termini fused with 6×His and their C termini fused with 3×flag or 3×myc tag. Each protein (about 1 μg) with the combinations indicated was incubated at 4°C for 3 h in the immunoprecipitation buffer. The protein complexes were precipitated with EZview Red Anti-c-Myc Affinity Gel, separated on 10% SDS-PAGE gels, and detected with the antibodies indicated. Asterisks indicate the OW76.1 protein. D, BiFC assay of OsWRKY62.1 and OsWRKY76.1 interactions. OW62.1 and OW76.1 were fused in frame with the YFP C-terminal region (YFP^C) or the YFP N-terminal region (YFP^N). The plasmids indicated were introduced into the leaf cells of *N. benthamiana* through agroinfiltration. Confocal images were taken at 72 h after infiltration. From left to right are YFP images, 4',6-diamino-phenylindole (DAPI) nuclear staining images, bright-field images (differential interference contrast [DIC]), and merged YFP, DAPI, and DIC images. Bars = 20 μm.
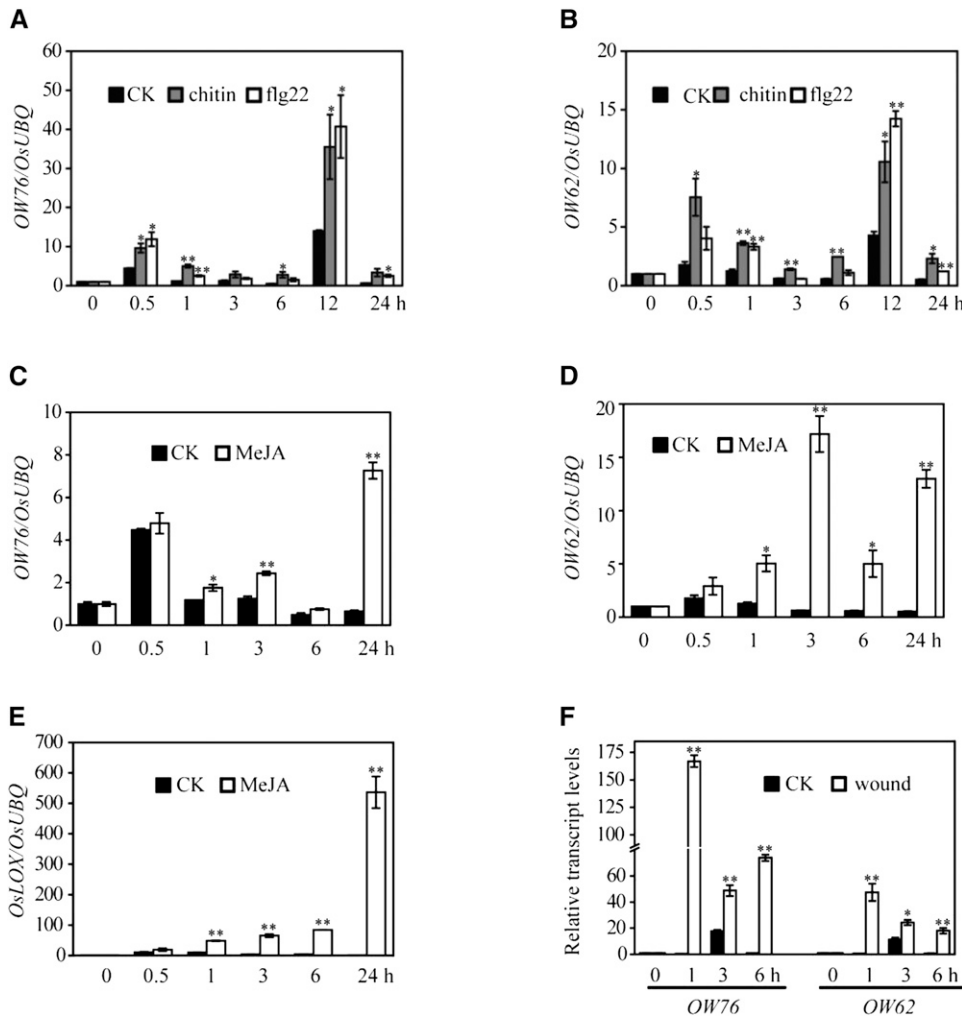
Figure 2. Expression profiles of the *OsWRKY62* and *OsWRKY76* genes in response to chitin, flg22, MeJA, and wounding. A to E, Rice seedlings were treated with 0.7 μM flg22, 10 nM chitin, or 100 μM MeJA in 10 mM MES (pH 6) buffer and sampled at the indicated time points. Mechanical wounding was performed on leaves of 3-week-old plants by crushing with a hemostat. F, Transcription levels expressed as the ratio to the level of transcript at 0 h using the rice *UBIQUITIN* (*OsUBQ*) gene as an internal standard. Values shown are means $\pm$ SE of three replicates. Statistically significance changes are indicated by asterisks: *, $P < 0.05$ and **, $P < 0.01$. CK, Mock treatment.

We subsequently generated a construct to down-regulate the expression of both genes (dsOW62/76) in rice by RNAi. Among the 11 independent transgenic lines obtained, some lines began to display dark brown spots on the oldest leaf about 2 weeks after sowing, and the spots gradually enlarged, coalesced, and eventually led to necrosis of the leaf (Fig. 5A). Cell death in the double RNAi plants was confirmed by Trypan Blue staining, showing that the older the leaf was, the more cell death occurred (Fig. 5B). The dsOW62/76 plants with leaf necrosis were dwarf and set fewer seeds than the wild-type plants (Fig. 5D). We also examined H_2O_2 accumulation by DAB staining in these lines, and the stain was obvious in leaves of dsOW62/76 plants but rarely observable in those from the control plants (Fig. 5C).

To evaluate the responses to pathogens, dsOW62/76 transgenic and control plants were inoculated with *M. oryzae* SZ. Disease symptoms developed on the wild-type ZH17 plants 5 d after inoculation, whereas hypersensitive response-like lesions emerged in the dsOW62/76 plants (Fig. 5E), and the levels of fungal DNA were hardly detectable in the dsOW62/76 lines (Fig. 5F). Similarly, disease lesions were much shorter in the dsOW62/76

transgenics challenged with *Xoo* J18 than that in the ZH17 control plants (Fig. 5, G and H). These results demonstrate that dsOW62/76 plants have enhanced resistance against both bacterial and fungal pathogens.

We analyzed the expression of defense-related genes by quantitative reverse transcription (qRT)-PCR. The levels of *PR1a*, *PR1b*, and *PR10* transcripts were increased significantly in the dsOW62/76 line compared with those in the ZH17 control (Fig. 5I). The expression of *PAL1*, encoding a key enzyme in the biosynthesis of phenolic compounds, was elevated about 30-fold in the RNAi line. CPS2 and CPS4 (for *ent*- and *syn*-copalyl diphosphate synthases 2 and 4) as well as CYP71Z7 and MAS are enzymes involved in the biosynthetic pathways of antimicrobial phytocassanes and momilactones, respectively (VanEtten et al., 1994; Otomo et al., 2004; Yokotani et al., 2013). The expression of these genes also was increased in the dsOW62/76 plant. Finally, we examined the accumulation of phytoalexins. As shown in Table I, dsOW62/76 plants accumulated much higher amounts of diterpenoid phytoalexins, including momilactones, phytocassanes, and flavonoid sakuranetin, compared with the ZH17 control

Figure 3. Histochemical analyses of OsWRKY62 and OsWRKY76 expression. *OsWRKY62.1* and *OsWRKY76.1* promoters were fused with the *GUS* gene, and the resultant plasmids (Cp-OW62p:Gus and Cp-OW76p:Gus) were transformed into rice calli. The T2 progeny of Cp-OW62p:Gus and Cp-OW76p:Gus were used for GUS activity staining. Seven-day-old seedlings (A), primary and lateral roots of 12-d-old plants (B), stem and the third node counted from the top at the reproductive stage (C), flowers (D), ligule base and leaf sheath at the reproductive stage (E), and immature seed (F) are shown. An image or a group of three images are shown from left to right as Cp-OW76p:Gus, wild-type Zhonghua 17 (ZH17), and Cp-OW62p:Gus. Bars = 1 mm (D), 5 mm (A, B, E, and F), and 1 cm (C).
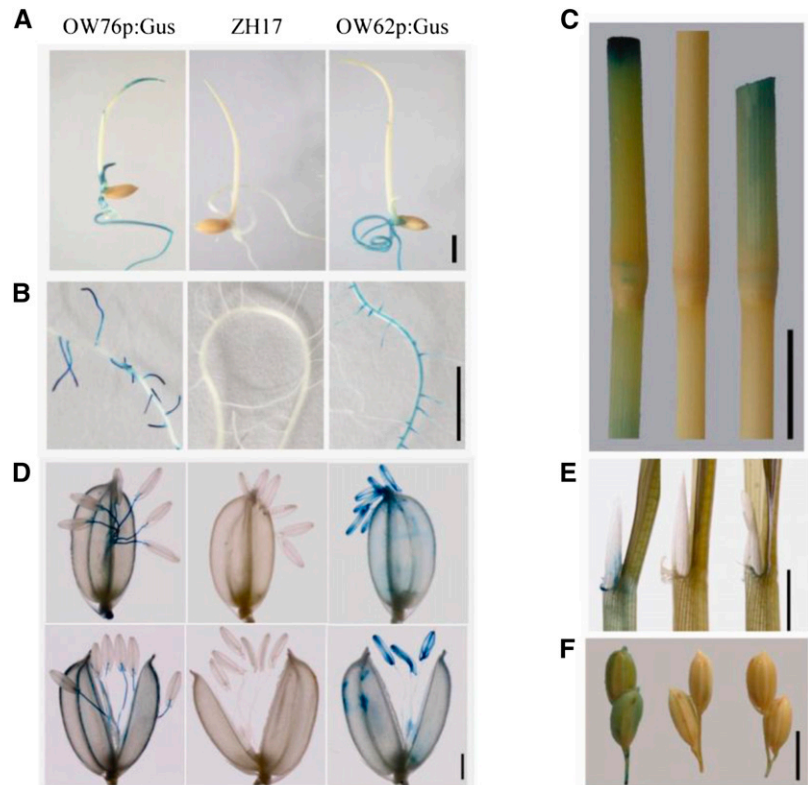
plants. We also generated plants that overexpress both full-length OsWRKY62.1 and full-length OsWRKY76.1 by crossing OW76.1ox and OW62.1ox lines. Plants overexpressing OsWRKY62.1 or OsWRKY76.1 and their hybrid F2 progeny had decreased levels of phytoalexins (Table I) and suppressed expression of defense-related genes that are induced by MeJA treatment (Supplemental Fig. S3) compared with the ZH17 control. These data demonstrate that the enhanced disease resistance in the RNAi plants was correlated to an enhanced expression of defense genes and phytoalexin accumulation, which is consistent with the conclusion that OsWRKY62.1 and OsWRKY76.1 are repressors of plant defense.

Alternative Splicing of *OsWRKY62* and *OsWRKY76* in the RNAi Plants of *OsWRKY76*

Our initial analysis of gene expression was based on qRT-PCR of the 3′ region, showing that the total transcript levels of *OsWRKY62* and *OsWRKY76* increased in the overexpressing plants and decreased in dsOW62 RNAi lines compared with the ZH17 plants (Fig. 6). Interestingly, the total transcript levels of both *OsWRKY62* and *OsWRKY76* increased greatly in the double RNAi lines. To further analyze the abnormal gene expression, we designed new sets of primers that amplify the entire open reading frames of the two genes. We discovered that both *OsWRKY62* and *OsWRKY76* were transcribed in two forms in the ZH17

plants (Fig. 6C). The *OsWRKY62.1* transcript encodes the full-length protein as annotated in the current genome database (http://rice.plantbiology.msu.edu). The alternative *OsWRKY62.2* transcript contains the first intron, which is lacking in *WRKY62.1*, so that the deduced OsWRKY62.2 protein is truncated due to a premature stop codon or the truncated protein is produced from an alternative translational start site after the retained intron (Supplemental Fig. S1). The *OsWRKY76.2* transcript is smaller than *OsWRKY76.1*, since it spliced a larger intron with differences at both splicing donor and acceptor sites (Supplemental Fig. S1). The deduced OsWRKY76.2 lacks part of the CC domain compared with OsWRKY76.1, and OsWRKY76.3 could be deduced after the remaining intron. We analyzed transcripts of two other *WRKY* genes of the IIa subgroup and found no alternative splicing in transcripts of *OsWRKY28* and *OsWRKY71* in dsOW62/76 plants (Supplemental Fig. S4). The increase of *OsWRKY62* expression in the dsOW76 and dsOW62/76 plants was caused mostly by the elevated abnormal transcripts (Fig. 6, C and D). The *OsWRKY62.2* transcript increased more than 20 times faster than *OsWRKY62.1*.

Next, we examined *OsWRKY62* transcripts by qRT-PCR using the rice samples inoculated with *M. oryzae* or treated with MeJA analyzed in Figure 2. As shown in Figure 6, E and F, the two *OsWRKY62* transcripts were induced by the fungal pathogens or treatment with MeJA; however, there was a shift in the ratio of
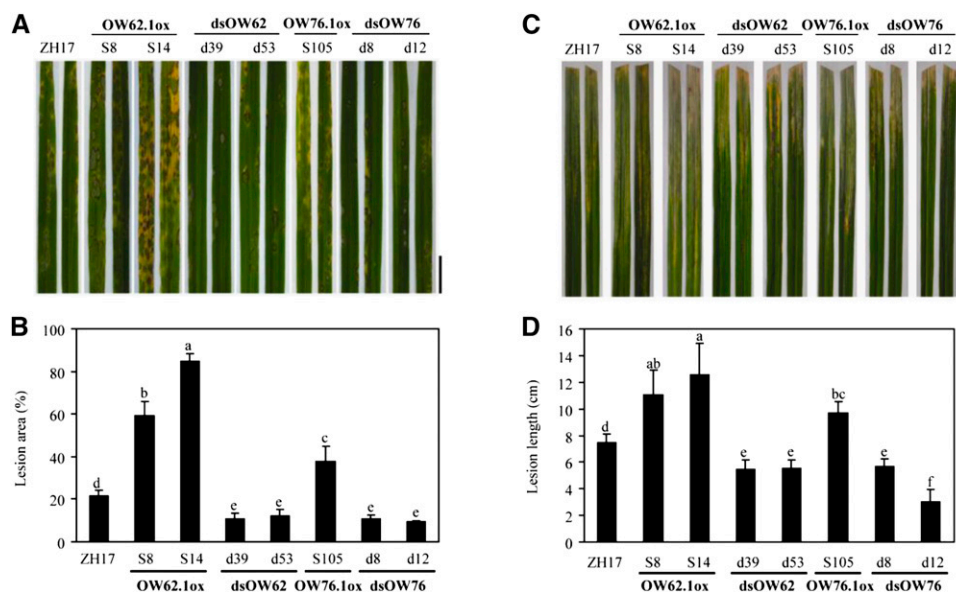
Figure 4. *OsWRKY62.1* and *OsWRKY76.1* play negative roles in resistance against rice blast and bacterial blight pathogens. A, Three-week old transgenic (T2 progeny) and wild-type (ZH17) plants were inoculated with *M. oryzae* SZ (5×10^5 conidia mL^{-1}) by foliar spraying. Photographs were taken 5 d after inoculation. B, Lesion areas are from inoculated leaves of 10 plants for each line. C, Six-week-old plants were challenged with *Xoo* isolate J18 using the leaf-clipping method. Photographs were taken 2 weeks after inoculation. D, Lesion lengths are averages of 10 leaves. Values marked with different letters indicate statistically significant differences as analyzed by the SAS software (Duncan's multiple range test, $\alpha = 0.05$). Results from a representative experiment are shown. The suffix ox is for *OsWRKY62.1*- and *OsWRKY76.1*-overexpressing plants, and the prefix ds is for RNAi lines. Bars = 1 cm (A) and 2 cm (C).

OsWRKY62.1 to *OsWRKY62.2*, due to a much greater increase in the production of the abnormal *OsWRKY62.2* transcript, relative to full-length *OsWRKY62.1*, especially after pathogen infection.

For *OsWRKY76*, a high GC-rich sequence (11 bp with 10 GCs: TCGCCGCCGCG) at the splicing sites of *OsWRKY76.2* exists in *OsWRKY76.1* and *OsWRKY76.3*. Consequently, it was not possible to design qRT-PCR primers to distinguish the alternative *OsWRKY76* transcripts. Therefore, we examined *OsWRKY76* transcripts by reverse transcription (RT)-PCR, as shown in Supplemental Figure S5. In the double RNAi lines, the abnormal transcripts (*OsWRKY76.2* and *OsWRKY76.3*) increased to higher levels than that of *OsWRKY76.1*. On the other hand, in *M. oryzae*-infected tissues, *OsWRKY76.1* transcript increased more than that of *OsWRKY76.2*. In MeJA-treated tissues, all transcripts increased to similar levels (Supplemental Fig. S5).

Analysis of the Loss-of-Function Knockout Mutants of *OsWRKY62* and *OsWRKY76*

To avoid potential complications regarding the conclusion of OsWRKY62 and OsWRKY76 as repressors of defense based exclusively on RNAi constructs, we made loss-of-function knockout (KO) mutants using the CRISPR/Cas9 technology (Miao et al., 2013). The homozygous W62-8-KO line carries a T insertion at the target site and causes a reading frame shift, whereas the W76-3-KO line is a biallelic mutant carrying an A insertion in one chromosome and a 17-bp deletion in the other chromosome (Supplemental Fig. S6). We found that levels of *OsWRKY62.1* and *OsWRKY62.2* transcripts increased in the W62-8-KO mutant, compared with the control line NT (a regenerated nontransgenic plant line). Similarly, levels of *OsWRKY76.1* and *OsWRKY76.2* transcripts were raised in W76-3-KO plants. Furthermore, the expression of *OsWRKY76.1* increased significantly in W62-8-KO mutant plants and levels of *OsWRKY62.1* and *OsWRKY62.2* transcripts were up-regulated in W76-3-KO plants, indicating that the levels of *OsWRKY62* and *OsWRKY76* were coregulated. These results were consistent with those observed in dsOW76 plants (Fig. 6) and more clearly showed that it was the loss of function of *OsWRKY62*/*OsWRKY76*, and not potential secondary effects of RNAi, that resulted in the up-regulation of their transcripts. In contrasts to plants overexpressing *OsWRKY62.1* and *OsWRKY76.1*, the W62-8-KO and W76-3-KO plants showed elevated expression of defense-related genes, accumulation of phytoalexins, and enhanced resistance against *M. oryzae* SZ (Fig. 7).

Interactions between Alternative Isoforms of OsWRKY62 and OsWRKY76

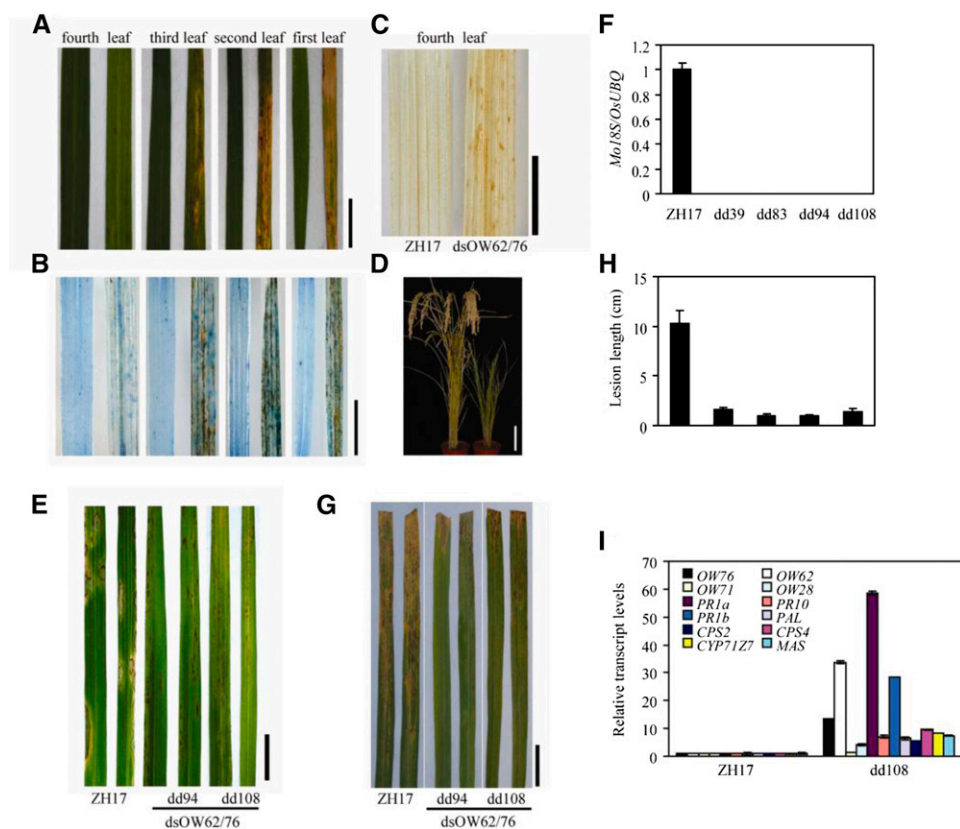The high-level accumulation of abnormal transcripts in pathogen-infected or dsOW62/76 RNAi plants

Figure 5. The *OsWRKY62/OsWRKY76* double RNAi plants showed spontaneous cell death and enhanced resistance against rice pathogens. A to D, Phenotypes of wild-type ZH17 (left) and the double RNAi line (dsOW62/76; right). A, Lesions on leaves of 3-week-old dsOW62/76 plants (dd108). B, Detection of cell death by Trypan Blue staining. C, Detection of hydrogen peroxide (H_2O_2) accumulation by 3,3'-diaminobenzidine (DAB) staining in the fourth leaves. D, Dwarfism of the dd108 plant. Leaves are counted from bottom to top. E and G, Transgenic (T2 progeny) and ZH17 plants were inoculated with *M. oryzae* SZ (E) or *Xoo* J18 (G), and disease was evaluated as described in Figure 4. F, The amount of fungal mass in inoculated leaves was estimated by qRT-PCR. Values are means ± SE of six leaves. H, Lesion lengths of transgenic and control plants. I, Total RNA was isolated from leaves of 3-week-old dd108 and control plants. Gene expression was determined by qRT-PCR using *OsUBQ* as the reference gene. Transcription levels are shown relative to ZH17 rice leaves. Values shown are means ± SE of three replicates. In F, H, and I, Differences between ZH17 and transgenic lines are significant ($P < 0.01$, Student's *t* test). Experiments were repeated three times with similar results. Bars = 1 cm (A–C and E), 2 cm (G), and 10 cm (D).

prompted us to investigate their functions. First, we analyzed the localization of GFP-fused OsWRKY62.2 and OsWRKY76.2 proteins and found that the alternative proteins had similar localization patterns to those of OsWRKY62.1 and OsWRKY76.1, respectively (Supplemental Fig. S7). In addition, OsWRKY62.2 and OsWRKY76.2 could form homocomplexes and heterocomplexes as assayed by BiFC (Supplemental Fig. S7).

Table I. *Accumulation of momilactone A and B, phytocassane A to E, and sakuranetin phytoalexins in various rice lines*

Each data point represents the relative abundance of lidocaine (0.05 ng in each sample) in the positive mode and [$^2H_6$]-ABSCISIC ACID (D_6ABA, 10 ng) in the negative mode. All of the compounds (ng g^{-1} dry weight) were detected in the positive mode except for sakuranetin. F2 is the hybrid of OW76.1ox-105 × OW62.1ox-14. Each data point represents the mean ± SE of two replicates. ND, Not determined.

| Plants	Momilactones		Phytocassanes					Sakuranetin
	A	B	A	B	C	D	E	
ZH17	0.14 ± 0.06	ND	ND	ND	ND	ND	ND	15.91 ± 1.30
dsOW76-3	65.66 ± 14.98	10.10 ± 2.30	7.68 ± 1.76	12.94 ± 2.96	11.36 ± 2.60	9.58 ± 2.18	11.26 ± 2.56	ND
dsOW76-8	41.54 ± 3.62	19.61 ± 0.70	5.22 ± 1.24	18.48 ± 0.92	9.24 ± 0.60	9.40 ± 0.44	12.62 ± 0.90	ND
dsOW62-39	16.52 ± 1.16	1.44 ± 0.16	0.96 ± 0.06	3.58 ± 0.26	1.78 ± 0.12	2.30 ± 0.16	2.20 ± 0.16	ND
dsOW62-53	6.10 ± 0.72	0.46 ± 0.06	0.16 ± 0.02	0.38 ± 0.06	0.10 ± 0.02	0.12 ± 0.02	0.12 ± 0.02	ND
dsOW62/76-94	367.92 ± 36.06	63.18 ± 5.56	48.92 ± 4.90	236.58 ± 22.00	70.54 ± 6.54	63.62 ± 6.04	389.30 ± 37.34	139.48 ± 7.02
dsOW62/76-108	675.85 ± 9.49	622.36 ± 6.06	185.57 ± 14.20	830.70 ± 74.42	216.34 ± 31.21	387.86 ± 10.15	933.94 ± 34.06	680.00 ± 16.00
OW76.1ox-105	ND	ND	ND	ND	ND	ND	0.02 ± 0.02	ND
OW62.1ox-14	0.02 ± 0.02	ND	ND	ND	ND	ND	ND	ND
F2	0.02 ± 0.01	ND	ND	ND	ND	ND	0.02 ± 0.02	ND
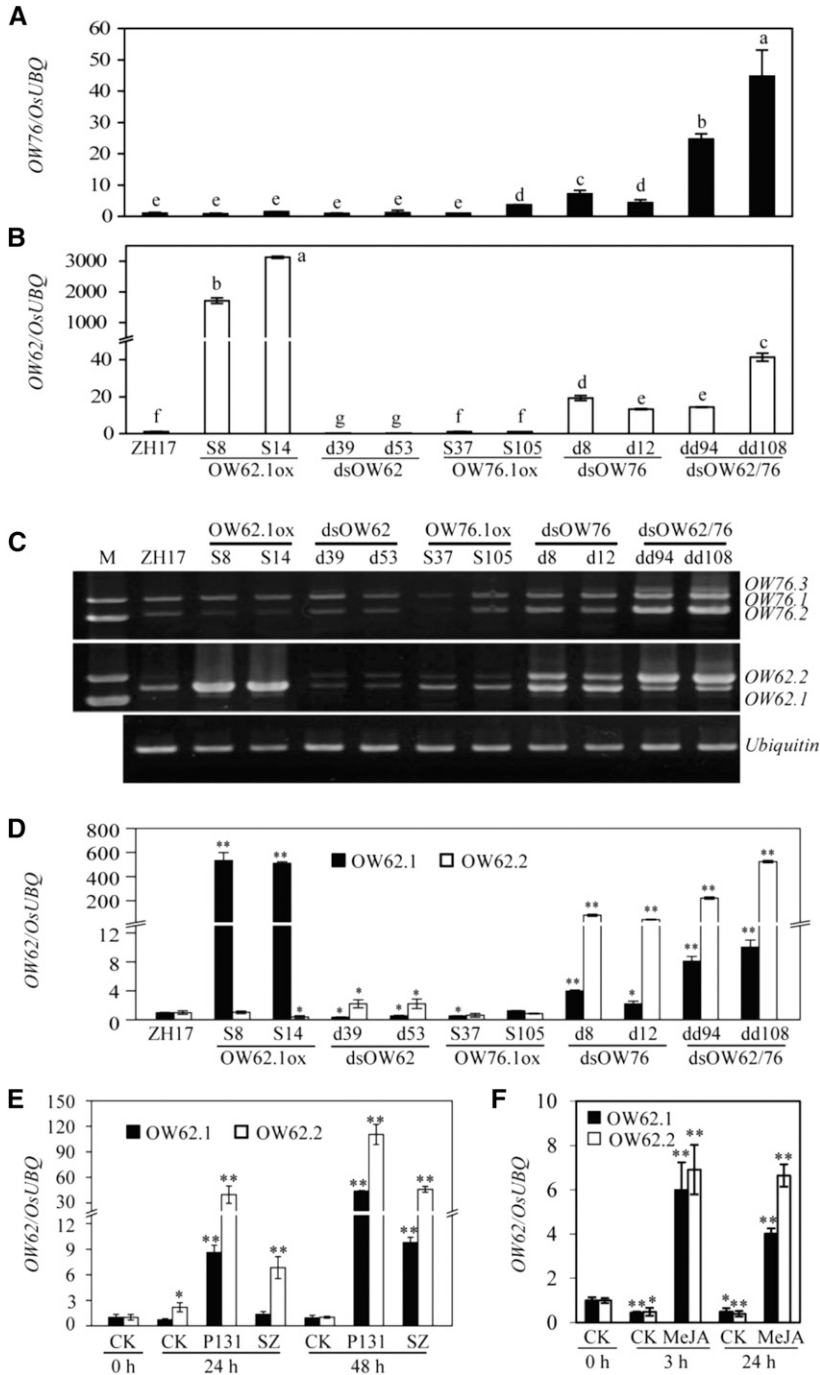
Figure 6. Changes in alternative transcript levels of *OsWRKY62* and *OsWRKY76* in the RNAi plants or plants after pathogen infection or MeJA treatment. A and B, Expression of *OsWRKY62* and *OsWRKY76* was analyzed by qRT-PCR using total RNA extracted from leaves of 3-week-old plants. Error bars indicate sᴇ (*n* = 3). Values marked with different letters indicate statistically significant differences as analyzed by the SAS software (Duncan's multiple range test, *α* = 0.05). C, *OsWRKY76.1* to *OsWRKY76.3* (*OW76.1–OW76.3*) and *OsWRKY62.1* and *OsWRKY62.2* (*OW62.1* and *OW62.2*) were obtained by RT-PCR amplification of complementary DNAs (cDNAs) from dd94 and dd108 plants. D to F, Levels of alternative transcripts *OsWRKY62.1* (*OW62.1*) and *OsWRKY62.2* (*OW62.2*) were analyzed by qRT-PCR in transgenic plants (D), after *M. oryzae* infection (E), or after MeJA treatment (F). Samples were collected from plants at the time points indicated after inoculation with a virulent (SZ) or avirulent (P131) strain of *M. oryzae* or after treatment with MeJA (0.1 mM, in 10 mM MES buffer, pH 6). CK, Mock treatment. Transcription levels are shown relative to the level of transcript at 0 h or those in wild-type ZH17 using the *OsUBQ* gene as an internal standard. Values shown are means ± sᴇ of three replicates. Statistically significance changes are indicated by asterisks: *, *P* < 0.05 and **, *P* < 0.01 (Student's *t* test).

In the yeast two-hybrid assays, OsWRKY76.2, which is truncated at the N terminus (Fig. 8A), had normal interaction patterns like OsWRKY76.1 (Fig. 8B, lanes 1–3). Similar interaction patterns were observed between OsWRKY62.1 and OsWRKY62.2 (Fig. 8B, lanes 4–6). Intriguingly, however, truncated OsWRKY62.2 and OsWRKY76.2 showed stronger interactions than their full-length counterparts (Fig. 8B, lanes 7 and 10). We conducted competitive protein interactions using the yeast three-hybrid system. As shown in Figure 8C, induction of truncated OsWRKY76.2 significantly decreased the interaction between full-length OsWRKY76.1 and full-length OsWRKY62.1. OsWRKY62.2 showed a relatively weaker effect on the OsWRKY76.1-OsWRKY62.1 interaction (Fig. 8C).

Analysis of the Transcriptional Repressor Activity of OsWRKY62.1 and OsWRKY76.1

WRKY transcription factors of the IIa subgroup are reported as transcription repressors (Peng et al., 2008; Chujo et al., 2013; Yokotani et al., 2013). Surprisingly,

Figure 7. *OsWRKY76* and *OsWRKY62* knockout plants exhibit enhanced defense responses. A, Levels of alternative transcripts of *OsWRKY76* and *OsWRKY62* were determined by RT-PCR analysis. The leaf samples were collected from 8-week-old knockout (KO) and regenerated nontransgenic (NT) plants. B, Transcript levels of defense genes were determined by qRT-PCR using rice *UBQ* as a reference. Expression levels in the knockout lines are shown relative to that in regenerated nontransgenic rice leaves. Values shown are means ± SE of three replicates. The amounts of momilactone A, phytocassanes B, and phytocassanes C were determined by liquid chromatography-tandem mass spectrometry using lidocaine as an internal standard. Data are means ± SE of two replicates. *, $P < 0.05$ and **, $P < 0.01$ (Student's *t* test). C, Detached leaves of 8-week-old plants were inoculated with *M. oryzae* SZ (1×10^5 spores mL^{-1}). Photographs were taken 6 d post inoculation. Lesion lengths are averages of 10 inoculated sections. Values marked with different letters indicate significant differences as analyzed by the SAS software (Duncan's multiple range test, $\alpha = 0.05$). Bar = 0.5 cm.
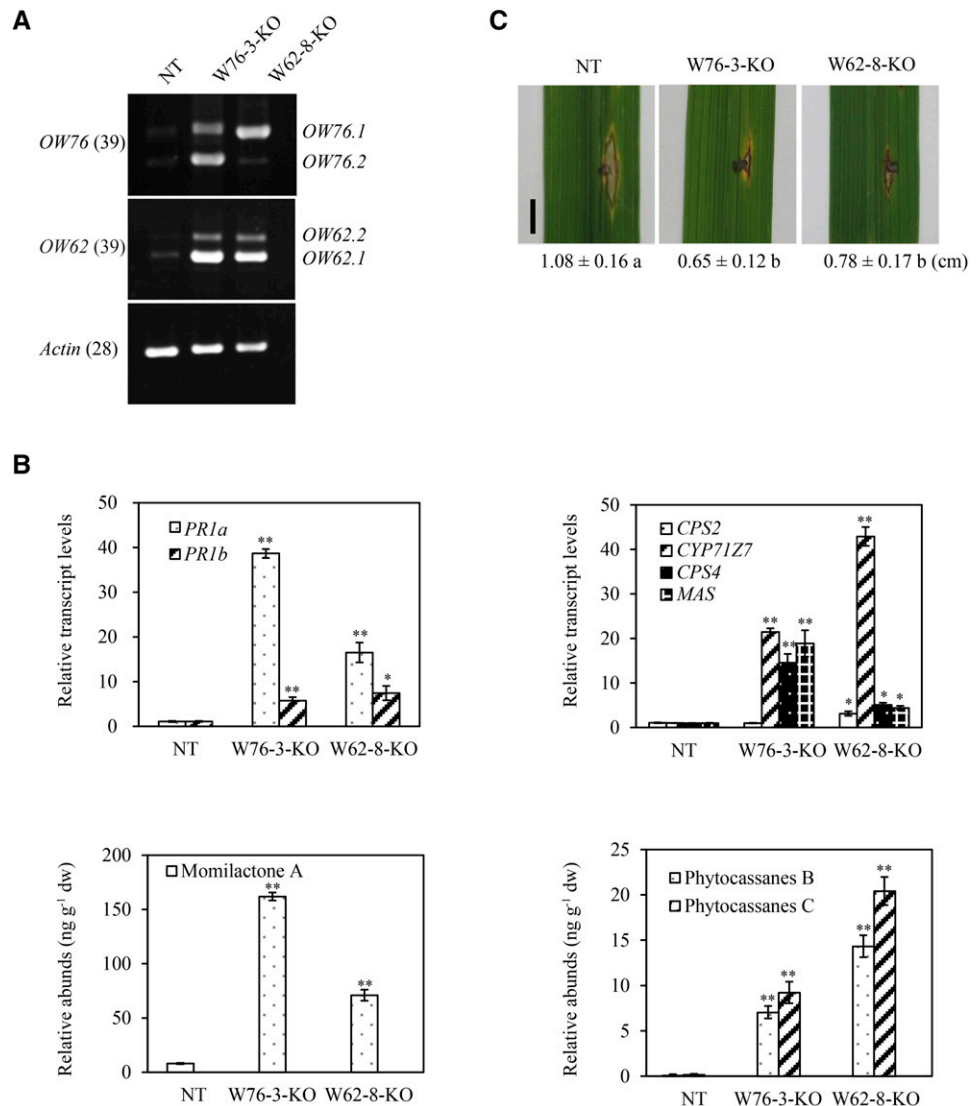
however, we observed that OsWRKY62.1 had a low level of autoactivation activity in yeast (Fig. 1B). This result prompted us to examine the transcription activity of the two WRKY TFs in planta. To increase the efficiency of transient assays, the pCambia 1301 vector was modified to put the reporter and the effector gene in the same plasmid (Fig. 9A). Plasmids were introduced into leaves of *N. benthamiana* by *A. tumefaciens*-mediated infiltration. OsWRKY76.1 (pWGus/W76.1) or OsWRKY76.2 (pWGus/W76.2) showed transcriptional repressor activity like OsWRKY62.1 (pWGus/W62.1; Fig. 9B). In contrast, OsWRKY62.2 (pWGus/W62.2), with the deletion of 39 amino acids at the N terminus of OsWRKY62.1, lost repressor activity (Fig. 9B). Most interestingly, the transcriptional repressor activity of full-length OsWRKY62.1 or OsWRKY76.1 did not change significantly with the addition of other splicing variant(s) except for OsWRKY62.2, which showed the greatest increase during pathogen infection, MeJA treatment, and dsOW62/76 RNAi plants (Figs. 6, D–F,

and 9C). This result suggests that OsWRKY62.2 could exert a strong dominant-negative effect on the functions of full-length OsWRKY62 and OsWRKY76 proteins in planta.

To further define the determinant repressor sequence in OsWRKY62.1, we performed serial deletions within the N-terminal 39-amino acid region of OsWRKY62.1 and measured the transcriptional activities of the resulting constructs in leaves of *N. benthamiana*. In initial experiments, the EDLEEK sequence was found to be required for the repressor activity of OsWRKY62.1, comparing the transcriptional activity of W62.1d29 and W62.1d35 (Fig. 9, D and E). However, the repressor activity of OsWRKY62.1 was not affected by a poly-Ala substitution mutation (W62.1m1) or a deletion (W62.1d1) that eliminates the EDLEEK sequence. This result implied that another sequence determinant in the N-terminal 39-amino acid region is involved in the transcriptional suppression. Indeed, further deletions and assays showed that the PTDDSAAAG sequence
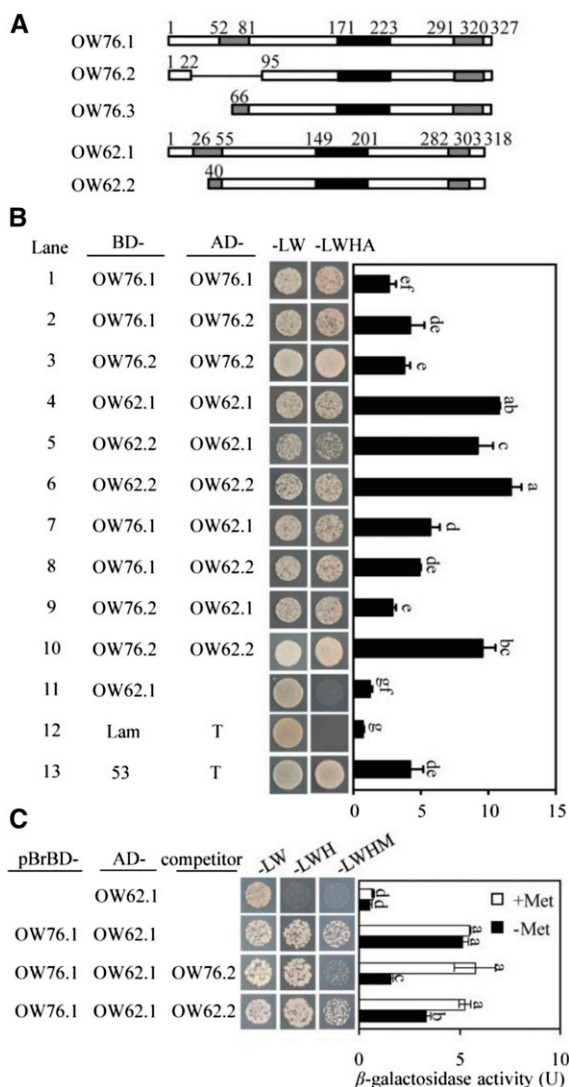
Figure 8. Interactions between alternatively spliced transcripts of OsWRKY76 and OsWRKY62. A, Schematic diagrams of OsWRKY62 and OsWRKY76 proteins. The domain is described in Figure 1. The amino acid positions correspond to those in the full-length proteins. B, Interactions among OW76.1, OW76.2, OW62.1, and OW62.2 in yeast two-hybrid assays. OW76.1, OW76.2, OW62.1, and OW62.2 were fused to the Gal4 DNA-binding domain (BD) and/or activation domain (AD). Yeast cells were incubated in SD medium lacking Leu and Trp (-LW; left) or Leu, Trp, His, and adenine (-LWHA; right) and photographed 3 d after plating. Yeast cells harboring AD-T with BD-53 or BD-Lam vector were used as the positive or negative control. C, Inhibition of interaction between OW76.1 and OW62.1 by OW76.2 or OW62.2. Yeast cells were incubated in SD medium lacking Leu and Trp (-LW; left), Leu, Trp, and His (-LWH; middle), or Leu, Trp, His, and Met (-LWHM; right) and photographed 3 d after plating. Yeast cells harboring BD with pAD-OW62.1 were used as a negative control. For β-galactosidase activity assays, three clones of each combination were grown in SD medium lacking Leu and Trp at 30°C to an optical density of 2 at 600 nm. In yeast-three hybrid assays, yeast colonies were grown in SD medium lacking Leu and Trp with (white) or without (black) Met at 30°C. The β-galactosidase activity was measured using O-nitrophenyl-β-D-galactopyranoside as the substrate. Experiments were repeated three times with similar results. Values marked with different letters indicate statistically significant differences (Duncan's multiple range test, α = 0.05).

also was required for the repressor activity of OsWRKY62.1 (Fig. 9, D and E). Taken together, our analyses revealed two sequence determinants, PTDDSAAAG and EDLEEK, in the N terminus of OsWRKY62.1 that are required for the repressor activity of OsWRKY62.1.

The N Termini Are Required for OsWRKY62 and OsWRKY76 Binding to the W Box in Vitro

We examined the DNA-binding activities of OsWRKY62 and OsWRKY76 by gel retardation assay. However, the recombinant full-length OsWRKY62 and OsWRKY76 proteins produced in *Escherichia coli* were insoluble and formed large aggregates of over 5,000 kD (Supplemental Fig. S8). Therefore, we made truncated versions of OsWRKY62.1 and OsWRKY76.1 that contain only the WRKY domain either with or without the N or C terminus. Among all the truncated versions, only glutathione *S*-transferase (GST)-OW62.1N and GST-OW76.1N that bear deletion at C termini produced multimers, as estimated by size-exclusion column chromatography (Supplemental Fig. S8). All other versions of proteins formed large aggregates, suggesting that OsWRKY76 and OsWRKY62 tend to self-aggregate, especially via the C-terminal part of the protein.

The soluble GST-OW62.1N and GST-OW76.1N proteins allowed us to perform gel-shift assays using a W box-containing sequence, 81P1, from the promoter of *OsWRKY76*. The specific binding of GST-OW62.1N or GST-OW76.1N to 81P1-B was confirmed (Fig. 10B). To determine whether the alternative splicing variants are affected in W box-binding activity, we expressed the equivalent parts of GST-OW62.2 (GST-OW62.2N) and GST-OW76.2 (GST-OW76.2N) proteins and performed gel-shift assays. We found that GST-OW62.2N had reduced W box-binding activity and that the binding of GST-OW76.2N to 81P1-B was hardly detectable (Fig. 10B). These results indicate that the N-terminal short sequences, which are missing in the alternative isoforms, are required for binding to a target promoter motif.

DISCUSSION

In this study, we characterized the structurally similar TFs OsWRKY76 and OsWRKY62 of the WRKY IIa subgroup in rice. Our results from transgenic overexpression and RNAi mutants support the general notion that this subgroup of WRKY TFs are transcriptional repressors that regulate basal and race-specific disease resistance in plants (Peng et al., 2008; Yokotani et al., 2013). In addition, we made two novel observations. First, protein-protein interaction and subcellular localization studies revealed that OsWRKY62 and OsWRKY76 can form a heterocomplex in the nucleus (Fig. 1D; Supplemental Fig. S7), suggesting that the two TFs may function collaboratively. Second, we discovered alternative splicing of the *OsWRKY62* and *OsWRKY76* transcripts. Most importantly, our further characterization shows a dominant-negative function of some of the
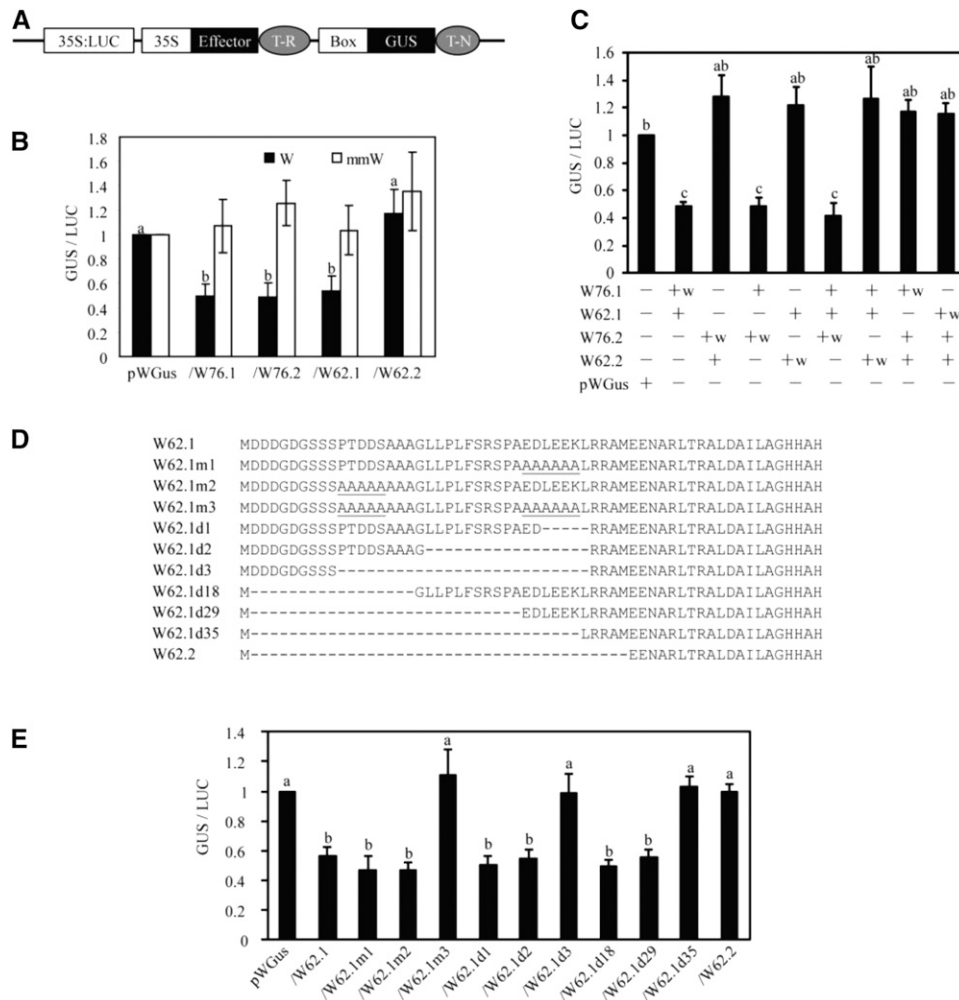
Figure 9. Transcription activities of OsWRKY62 and OsWRKY76 in planta. A, Schematic diagram of effector and reporter plasmids used in the transient expression assays. Box indicate DNA sequences containing the W box (W) or mutated W box (mmW); T-R, terminator of the rice *rbcS* gene; T-N, terminator of the *NOS* gene. B, C, and E, An effector gene could be inserted in the position of the effector shown in A. In the case of multiple effectors, the effector gene in the same plasmid with the W box is shown as +w, whereas the additional effector gene was constructed in a separate plasmid without the W box or *LUCIFERASE* (*LUC*) gene. The construct was introduced into leaves of *N. benthamiana* by agroinfiltration. Total proteins were extracted from the leaves 2 d after infiltration. GUS activity was normalized with LUC activity. A slash (/) indicates the presence of effector in the pWGus plasmid, and pWGus is without the effector gene. Data are means ± sᴇ of at least five independent experiments. Values marked with different letters indicate statistically significant differences as analyzed by the SAS software (Duncan's multiple range test, $\alpha = 0.05$). In E, the wild-type and mutated *OsWRKY62* genes were inserted in the position marked as effector shown in A. D, Amino acid sequence of the N-terminal region of OsWRKY62.1. Schematic diagrams of deletion (d1, d2, d3, d18, d29, d35) and poly-Ala substitution (m1, m2, and m3) mutants of OsWRKY62.1 (W62.1) are shown. Dashes represent deleted amino acids. The underlined letters represent the mutation sites.

truncated splice variants, revealing an example of alternative splicing-mediated feedback regulation for the WRKY family of TF genes.

Previously, *OsWRKY62* and *OsWRKY76* were shown to be induced by infection with *M. oryzae* (Ryu et al., 2006; Shimono et al., 2007) and by chitin treatment using suspension-cultured rice cells (Chujo et al., 2013). In this study, we found that both *OsWRKY62* and *OsWRKY76* were induced by not only PAMPs (chitin and flg22) but also by wounding and MeJA (Fig. 2). These data

suggest that *OsWRKY62* and *OsWRKY76* can integrate different biotic stress signals to regulate plant defense responses.

Xu et al. (2006) previously showed physical interactions among members of the Arabidopsis WRKY IIa subgroup. In particular, it has been shown that heterodimeric protein-protein interactions may alter the DNA-binding activity of WRKY TFs, although the specificity of DNA binding is not changed in vitro. For instance, the addition of AtWRKY60 enhances the binding of

A 81P1: 5'-TCG<u>TGAC</u>GTGCGCTCC<u>GTGAC</u>GTCGTCT<u>TGAC</u>CG-3'

B

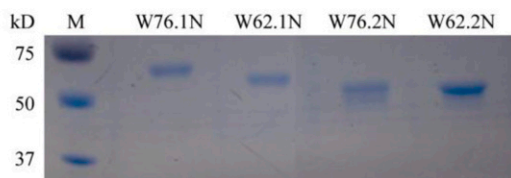|									
GST	+	−	−	−	−	−	−	−	−
OW76.1N	−	+	+	−	−	−	−	−	−
OW62.1N	−	−	−	+	+	−	−	−	−
OW76.2N	−	−	−	−	−	+	+	−	−
OW62.2N	−	−	−	−	−	−	−	+	+
81P1-B	+	+	+	+	+	+	+	+	+
81P1	−	−	50×	−	50×	−	50×	−	50×
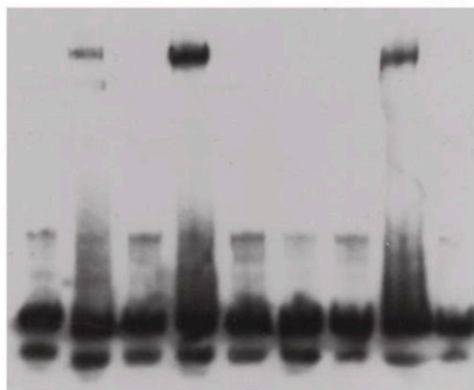
C

Figure 10. Binding of the N termini of OsWRKY76 and OsWRKY62 to the W box element in the promoter of *OsWRKY76*. A, Nucleotide sequence of 81P1 used in DNA-binding experiments, with the core W box sequences underlined. B, OW76.1N, OW76.2N, OW62.1N, and OW62.2N represent the GST-tagged recombinant proteins of OsWRKY76.1N (amino acids 1–230, C-terminal 97 amino acids deleted), OsWRKY76.2N (amino acids 1–158, C-terminal 97 amino acids deleted), OsWRKYW62.1N (amino acids 1–205, C-terminal 113 amino acids deleted), and OsWRKY62.2N (amino acids 1–166, C-terminal 113 amino acids deleted), respectively. 81P1-B, Biotin-labeled 81P1; 50×, addition of 50-fold unlabeled 81P1; +, presence; −, absence. The reaction mixture was separated on a native PAGE gel and blotted on a nylon membrane. The 81P1-B probe was detected by anti-biotin antibody. C, Loading control indicating the amounts of proteins used in the DNA-binding assay, stained by Coomassie Brilliant Blue. M, Protein molecular weight markers.

AtWRKY18 to the W box, whereas the binding activity of AtWRKY40 is reduced in the presence of AtWRKY60 (Xu et al., 2006). AtWRKY18, AtWRKY40, and AtWRKY60 also have been reported to cooperatively bind to the promoters of *ABI4* and *ABI5* to suppress their expression (Liu et al., 2012b). Using BiFC, yeast two-hybrid, and pull-down assays, we found that OsWRKY62 and OsWRKY76 could form both homocomplexes and heterocomplexes in the nucleus (Figs. 1 and 8; Supplemental Fig. S7). This is intriguing, considering that OsWRKY62 itself is localized to an unknown intracellular structure/organelle but is detected in the nucleus when coexpressed with OsWRKY76. Thus, the

nuclear function of OsWRKY62 likely depends on heterocomplex formation with OsWRKY76. It remains to be determined how the homocomplex and heterocomplex formation of OsWRKY62 and OsWRKY76 influences their collective transcriptional repressor activities in planta.

A previous study aimed at knocking down all four rice *WRKY* IIa genes yielded an unexpected observation that the RNAi plants had increased expression of the four genes and enhanced resistance to *Xoo* (Peng et al., 2010). However, the nature of the transcript increase of *OsWRKY62* and *OsWRKY76* in the RNAi plants remained elusive. We found that the increased transcripts in the dsOW76 and dsOW62/76 plants were due mainly to an enhanced production of alternatively spliced isoforms that are predicted to produce abnormal proteins (Fig. 6). The deduced OsWRKY62.2 and OsWRKY76.2 proteins from these alternatively spliced variants carry a partial or complete loss of the N-terminal CC domain (Fig. 7; Supplemental Fig. S1) and have reduced W box-binding activity (Fig. 10). The lack of the CC domain may influence the ability of OsWRKY62.1 and OsWRKY76.1 to interact with other regulatory factors or the basal transcription machinery. Therefore, production of the truncated forms of proteins may represent an important layer of feedback regulation to restrain the transcriptional repressor activities of OsWRKY62.1 and/or OsWRKY76.1, possibly through a dominant-negative mechanism, to allow for the full activation of WRKY-mediated defense responses. Indeed, we found that OsWRKY62.2 greatly affects the transcriptional activities of OsWRKY62.1 and OsWRKY76.1 (Fig. 9), and importantly, the dominant-negative OsWRKY62.2 transcript is preferentially increased during pathogen infection and MeJA treatment (Fig. 6, E and F). In addition, alternatively spliced transcripts of *OsWRKY62* and *OsWRKY76* were up-regulated in the W62-8-KO and W76-3-KO knockout plants (Fig. 7A). Feedback regulation via the production of alternatively spliced forms has emerged as an important layer of gene regulation in plants (Reddy et al., 2013; Staiger and Brown, 2013; Yang et al., 2014). The tobacco (*Nicotiana tabacum*) disease resistance *N* gene confers resistance to *Tobacco mosaic virus* (TMV; Whitham et al., 1994). Upon TMV infection, the transcript encoding a truncated protein was induced at a greater level than the transcript encoding the functional N protein (Dinesh-Kumar and Baker, 2000). The alternative transcript was found to be required for full resistance to TMV. In Arabidopsis, CIRCADIAN CLOCK-ASSOCIATED1 (CCA1) has a splicing variant, CCA1β, that lacks the DNA-binding MYB domain at the N terminus (Seo et al., 2012). CCA1β forms nonfunctional heterodimers with reduced DNA-binding activity and interferes with the formation of CCA1 and LATE ELONGATED HYPOCOTYL dimers that are required for their repressive effect on gene transcription. CCA1β functions as a dominant-negative inhibitor. In jasmonic acid (JA) signaling, the JAZ transcriptional repressor genes also undergo alternative splicing to restrain JA

signaling through the JA-induced production of truncated dominant-negative forms (Chung et al., 2010). To our knowledge, this study provides the first evidence for the constitutive and induced production of alternative splicing variants of WRKY TFs and their dominant-negative effects on the repressor function of full-length proteins during the plant defense response.

Although we have shown that full-length OsWRKY62.1 and OsWRKY76.1 are transcriptional repressors (Fig. 9), analyses of OsWRKY62.1 and OsWRKY76.1 sequences did not reveal any typical repressor motifs, such as the ERF-associated amphiphilic repression motif (Ohta et al., 2001; Kagale and Rozwadowski 2011). We found that the N-terminally truncated splice form OsWRKY62.2 has no repressor activity, indicating that the first 39 amino acids rich in acidic amino acids is required for OsWRKY62.1's transcriptional repressor activity in planta. Through deletion and mutation analyses, we found that two short sequences, PTDDS and EDLEEK, in the N terminus were required for the repressor activity of OsWRKY62.1 (Fig. 9, D and E). In addition, the N termini of OsWRKY62 and OsWRKY76 are required for binding to the W box promoter sequence in vitro (Fig. 10B). It is possible that PTDDS and EDLEEK represent new types of repression motifs. However, further research is needed to precisely identify the amino acid residues responsible for the repressor activity of OsWRKY62. Furthermore, since the N-terminally truncated alternative splice variants are reduced in their ability to bind the W box, and they have strong physical interactions with the full-length proteins (Fig. 8), we speculate that the dominant-negative effect of some of the alternative splice variants (Figs. 8 and 9) is more likely mediated through protein-protein interactions than through interference with the promoter-binding activity of full-length proteins.

MATERIALS AND METHODS

Plant Growth and Pathogen Inoculation

Transgenic rice (*Oryza sativa*) plants of T2 progeny were selected on one-half-strength Murashige and Skoog medium containing 60 mg L^{-1} hygromycin for 5 d and then transplanted to soil and grown in a greenhouse around 28°C under natural light conditions. Wild-type ZH17 *japonica* plants were used as the control. Three-week-old rice plants were inoculated with virulent *Magnaporthe oryzae* SZ by spraying the spore suspension (5×10^5 spores mL^{-1} containing 0.02% Silwet L-77) as described by Wang et al. (2007). The severity of infection was evaluated as described by Fukuoka et al. (2009). The qRT-PCR quantification of *M. oryzae* DNA was performed using primers from *M. oryzae* 18S ribosomal DNA and the rice *UBIQUITIN* gene, and infected leaves were collected 5 d post inoculation. For gene transcription analysis, 3-week-old ZH17 plants were inoculated with virulent *M. oryzae* SZ or avirulent P131 by spraying the spore suspension, and the leaves were sampled at the indicated time points.

To test the effect of the transgene on bacterial blight pathogen, 6-week-old rice plants were inoculated with *Xoo* J18 (optical density at 600 nm = 0.8) by the leaf-clipping method. Disease severity was estimated by measuring lesion length 2 weeks after infection.

Plant Treatments

Wild-type ZH17 seeds were surface sterilized and grown on one-half-strength Murashige and Skoog medium. Four-day-old seedlings were submerged in 10 mM MES (pH 6) buffer containing 100 μM MeJA, 0.7 μM flg22, or 10 nM chitin. Mechanical wounding was performed on leaves of seedlings by crushing with a hemostat.

Vector Construction and Rice Transformation

The coding sequences of *OsWRKY76.1* and *OsWRKY62.1* were amplified from ZH17 cDNA. The primers used for vector construction are listed in Supplemental Table S1. The sequence of *OsWRKY62.1* or *OsWRKY76.1* was fused with a *flag* tag and put under the control of a maize *UBIQUITIN* promoter to generate an overexpression construct (CDU-OW62.1 or CDU-OW76.1) as described previously (Liu et al., 2012a). To obtain the *OsWRKY76* or *OsWRKY62* RNAi vector, a 190-bp fragment of *OsWRKY76* or a 320-bp fragment of *OsWRKY62* was put under the control of a 35S promoter to form a hairpin structure after transcription. For simultaneous suppression of the two genes, the same RNAi fragments of *OsWRKY62* and *OsWRKY76* were ligated in tandem and then constructed to generate the double RNAi construct (35S:dsOW62/76).

To examine temporal and spatial expression, the promoter region of *OsWRKY62.1* or *OsWRKY76.1* (about 2 kb upstream of the translational start site) was fused with the *GUS* gene in pCambia 1301 vector. To analyze protein subcellular localization, the coding regions of *OsWRKY62* and *OsWRKY76* were fused with the *GFP* gene and driven by the 35S promoter, respectively.

All of the plasmids constructed were verified by sequencing and introduced into *Agrobacterium tumefaciens* EHA105 for rice transformation. The transgenic plants were obtained from immature seeds of ZH17 by the *A. tumefaciens*-mediated transformation method. Transgenic plants were selected by PCR amplification, and positive plants of T2 or higher progeny were used in the experiments unless indicated.

Transcriptional Activity Assay

A DNA fragment containing W boxes or their mutants was put immediately upstream of the 35S minimal promoter (from −46 to +10) controlled *GUS* gene (pWGus). A transcription factor gene to study could be constructed in the above plasmid with a *LUC* gene in it as an internal standard. GUS activities were determined 48 h after agroinfiltration.

RT-PCR and qRT-PCR Analyses

Total RNA of various tissues was isolated and treated with DNase I to remove possible DNA contaminations. Two micrograms of total RNAs was reverse transcribed using Moloney murine leukemia virus reverse transcriptase and random hexamers plus oligo d(T)$_{15}$ (Takara). The relative transcript levels were quantified using SYBR Green PCR MasterMix (Takara) and performed in a StepOne Quantitative PCR system (Applied Biosystems). Gene-specific primers used in qRT-PCR are listed in Supplemental Table S2. The *UBIQUITIN* gene was used as an internal control. To examine different transcripts, primers of *OsWRKY62* and *OsWRKY76* were designed to cover the open reading frame regions and listed in Supplemental Table S2. The band intensity of RT-PCR-amplified coding sequences was estimated by AlphaImager 2200 software.

Histochemical Staining

The accumulation of H$_2$O$_2$ was detected by DAB staining using the method described (Thordal-Christensen et al., 1997). Rice leaves were immersed in 1 mg mL^{-1} DAB for 10 h at room temperature. Dead cells of rice leaves were stained by using lactophenol-Trypan Blue solution according to the protocol reported (Yuan et al., 2007). The dsOW62/76 of T2 progeny and ZH17 plants were grown for 3 weeks in the conditions described above and used for staining. Photographs were taken after decolor treatment of the stained leaves.

For histochemical GUS analysis, whole seedlings or various tissues at different stages of development were collected for the detection of GUS activity.

Yeast Two- and Three-Hybrid Assays

The DNA fragments were inserted into the pGBKT7 plasmid to generate bait vectors and into pGADT7 plasmid to generate prey vectors. Yeast cells containing various combinations of bait and prey constructs were grown on SD medium lacking Leu and Trp for 4 d and then transferred to medium deficient of Leu, Trp, His, and adenine and grown further at 30°C for 3 d.

OsWRKY76.1 was cloned to fuse with the GAL4 DNA-binding domain in pBridge vector (Clontech). *OsWRKY62.2* or *OsWRKY76.2* was put under the control of the Met-repressible pMET25 promoter in the pBridge vector obtained above. The constructed plasmids combined with AD-OW62.1 vector were cotransformed into AH109 cells. The colonies were streaked on medium lacking Leu, Trp, and His supplemented with or without Met and grown at 30°C for 3 d.

β-Galactosidase activity was determined with yeast cells harboring different plasmid combinations grown in liquid SD medium without Leu and Trp using *O*-nitrophenyl β-D-galactopyranoside as the substrate according to the manufacturer's manual (Clontech). In the case of yeast three-hybrid assays, β-galactosidase activity was determined in SD medium lacking Leu and Trp with or without Met.

BiFC

Nicotiana benthamiana plants were grown in a greenhouse at 23°C with a 16-h/8-h light/dark cycle. BiFC assays were performed in leaves of *N. benthamiana* as described (Walter et al., 2004). *OsWRKY62* and *OsWRKY76* were cloned to fuse with YFP^N (N-terminal YFP) and/or YFP^C (C-terminal YFP). The combined plasmids were introduced into the leaves of 4-week-old *N. benthamiana* by agroinfiltrations. YFP fluorescence was visualized with a confocal laser scanning microscope (Eclipse TE2000; Nikon).

Expression of Recombinant Proteins and Pull-Down Assays

To express OsWRKY62.1, OsWRKY76.1, or their deletion proteins, the corresponding cDNAs were inserted into pGEX-4T-3 or pET-30a vector with the modification of introducing 3×myc or 3×flag at the C terminus of the recombinant protein and transformed into *Escherichia coli* BL21 (DE3). The recombinant proteins were purified using nickel-nitrilotriacetic acid agarose or Glutathione Sepharose 4B (GE Healthcare) based on the tag used.

For pull-down assays, the combinations of the fusion proteins tagged with 3×myc or 3×flag (1 μg each) were incubated with EZview Red Anti-c-Myc Affinity Gel (E6654; Sigma) for 3 h at 4°C. The beads were washed five times with the IP buffer (50 mM Tris-HCl, pH 7.4, 150 mM NaCl, 1 mM EDTA, and 0.1% [v/v] Triton X-100) and then resuspended in 2× SDS-PAGE loading buffer. The immunocomplexes were separated on a 10% polyacrylamide gel and probed with anti-flag or anti-myc antibody (Sigma), respectively.

EMSA

Recombinant proteins of 6×His-tagged or GST-tagged deletion mutants of OsWRKY62 and OsWRKY76 were expressed in *E. coli* and purified as described above. To investigate the potential interaction between the expressed proteins and the W box element, EMSA experiments were performed using 3′ biotin-labeled 81P1 oligonucleotide. The sequence of 81P1 was derived from the promoter region of *OsWRKY76*. Assay reaction proceeded at 25°C for 20 min before being electrophoresed on a 6% native polyacrylamide gel and then transferred onto a nylon membrane for western blot using anti-biotin antibody.

Phytoalexin Determination

The leaves sampled were freeze dried and extracted with 90% aqueous methanol containing 0.1% formic acid and internal standards of 10 ng of [^{2}H$_6$]-ABSCISIC ACID (D$_6$ABA) and 0.05 ng of lidocaine, then vigorously shaken for 12 h at 4°C. After centrifugation, the supernatant was transferred to a new 2-mL tube, and the pellets were extracted again with 0.6 mL of extraction buffer for 2 h at 4°C. The combined supernatants were concentrated by nitrogen gas, and the residues were dissolved in 0.1 mL of 90% aqueous ethanol containing 0.1% formic acid for liquid chromatography-tandem mass spectrometry.

Chemicals were separated by a C$_{18}$ column (2.1 × 150 mm, 3 μm; Phenomenex) on an Agilent 1260 separation module (Agilent). The identities of phytoalexins were confirmed by analysis of the ion fragments obtained by electrospray ionization mass spectrometry, with a source voltage of 3.2 kV in negative mode and 3 kV in positive mode and source temperature of 340°C. All of the phytoalexins were analyzed in the positive mode except sakuranetin. The phytoalexin levels were determined with the mass-to-charge ratio combinations (precursor/product ions) of 315.1955/271.2042 for momilactone A, 331.1904/269.19 for momilactone B, 317.2118/299.2006 for phytocassanes A, D, and E, 335.2217/317.2268 for phytocassane B, 319.2268/301.2162 for phytocassane C, and 285.0898/165.0165, 119.0466 for sakuranetin.

Supplemental Data

The following supplemental materials are available.

Supplemental Figure S1. Sequence comparison of OsWRKY62 and OsWRKY76 splicing variants.

Supplemental Figure S2. Localization of OsWRKY62.1 and OsWRKY76.1.

Supplemental Figure S3. Overexpression of *OsWRKY62.1* and *OsWRKY76.1* decreases the expression of *PR10* and phytoalexin synthesis genes with MeJA treatment.

Supplemental Figure S4. Expression of *OsWRKY28* and *OsWRKY71* in dsOW62/76 plants.

Supplemental Figure S5. Analyses of alternative transcripts of *OsWRKY76*.

Supplemental Figure S6. Sequence information of OsWRKY62 and OsWRKY76 in knockout mutant rice.

Supplemental Figure S7. Physical interaction between OsWRKY62.2 and OsWRKY76.2.

Supplemental Figure S8. Chromatograms of OsWRKY62 and OsWRKY76 recombinant proteins.

Supplemental Table S1. Primers used in vector construction.

Supplemental Table S2. Gene-specific primers for PCR detection.

LITERATURE CITED

Agarwal P, Reddy MP, Chikara J (2011) WRKY: its structure, evolutionary relationship, DNA-binding selectivity, role in stress tolerance and development of plants. Mol Biol Rep **38:** 3883–3896

Bakshi M, Oelmüller R (2014) WRKY transcription factors: jack of many trades in plants. Plant Signal Behav **9:** e27700

Chang C, Yu D, Jiao J, Jing S, Schulze-Lefert P, Shen QH (2013) Barley MLA immune receptors directly interfere with antagonistically acting transcription factors to initiate disease resistance signaling. Plant Cell **25:** 1158–1173

Chujo T, Kato T, Yamada K, Takai R, Akimoto-Tomiyama C, Minami E, Nagamura Y, Shibuya N, Yasuda M, Nakashita H, et al (2008) Characterization of an elicitor-induced rice WRKY gene, *OsWRKY71*. Biosci Biotechnol Biochem **72:** 240–245

Chujo T, Miyamoto K, Shimogawa T, Shimizu T, Otake Y, Yokotani N, Nishizawa Y, Shibuya N, Nojiri H, Yamane H, et al (2013) OsWRKY28, a PAMP-responsive transrepressor, negatively regulates innate immune responses in rice against rice blast fungus. Plant Mol Biol **82:** 23–37

Chung HS, Cooke TF, Depew CL, Patel LC, Ogawa N, Kobayashi Y, Howe GA (2010) Alternative splicing expands the repertoire of dominant JAZ repressors of jasmonate signaling. Plant J **63:** 613–622

Dinesh-Kumar SP, Baker BJ (2000) Alternatively spliced *N* resistance gene transcripts: their possible role in tobacco mosaic virus resistance. Proc Natl Acad Sci USA **97:** 1908–1913

Fu ZQ, Dong X (2013) Systemic acquired resistance: turning local infection into global defense. Annu Rev Plant Biol **64:** 839–863

Fukuoka S, Saka N, Koga H, Ono K, Shimizu T, Ebana K, Hayashi N, Takahashi A, Hirochika H, Okuno K, et al (2009) Loss of function of a proline-containing protein confers durable disease resistance in rice. Science **325:** 998–1001

Hayashi N, Inoue H, Kato T, Funao T, Shirota M, Shimizu T, Kanamori H, Yamane H, Hayano-Saito Y, Matsumoto T, et al (2010) Durable panicle blast-resistance gene *Pb1* encodes an atypical CC-NBS-LRR protein and was generated by acquiring a promoter through local genome duplication. Plant J **64:** 498–510

Inoue H, Hayashi N, Matsushita A, Xinqiong L, Nakayama A, Sugano S, Jiang CJ, Takatsuji H (2013) Blast resistance of CC-NB-LRR protein Pb1 is mediated by WRKY45 through protein-protein interaction. Proc Natl Acad Sci USA **110:** 9577–9582

Ishihama N, Yamada R, Yoshioka M, Katou S, Yoshioka H (2011) Phosphorylation of the *Nicotiana benthamiana* WRKY8 transcription factor by MAPK functions in the defense response. Plant Cell **23:** 1153–1170

Jones JD, Dangl JL (2006) The plant immune system. Nature **444:** 323–329

Kagale S, Rozwadowski K (2011) EAR motif-mediated transcriptional repression in plants: an underlying mechanism for epigenetic regulation of gene expression. Epigenetics **6:** 141–146

Liu D, Chen X, Liu J, Ye J, Guo Z (2012a) The rice ERF transcription factor *OsERF922* negatively regulates resistance to *Magnaporthe oryzae* and salt tolerance. J Exp Bot **63:** 3899–3911

Liu X, Bai X, Wang X, Chu C (2007) OsWRKY71, a rice transcription factor, is involved in rice defense response. J Plant Physiol **164:** 969–979

Liu ZQ, Yan L, Wu Z, Mei C, Lu K, Yu YT, Liang S, Zhang XF, Wang XF, Zhang DP (2012b) Cooperation of three WRKY-domain transcription factors WRKY18, WRKY40, and WRKY60 in repressing two ABA-responsive genes *ABI4* and *ABI5* in *Arabidopsis*. J Exp Bot **63:** 6371–6392

Mao G, Meng X, Liu Y, Zheng Z, Chen Z, Zhang S (2011) Phosphorylation of a WRKY transcription factor by two pathogen-responsive MAPKs drives phytoalexin biosynthesis in *Arabidopsis*. Plant Cell **23:** 1639–1653

Miao J, Guo D, Zhang J, Huang Q, Qin G, Zhang X, Wan J, Gu H, Qu LJ (2013) Targeted mutagenesis in rice using CRISPR-Cas system. Cell Res **23:** 1233–1236

Ohta M, Matsui K, Hiratsu K, Shinshi H, Ohme-Takagi M (2001) Repression domains of class II ERF transcriptional repressors share an essential motif for active repression. Plant Cell **13:** 1959–1968

Otomo K, Kenmoku H, Oikawa H, König WA, Toshima H, Mitsuhashi W, Yamane H, Sassa T, Toyomasu T (2004) Biological functions of *ent-* and *syn-*copalyl diphosphate synthases in rice: key enzymes for the branch point of gibberellin and phytoalexin biosynthesis. Plant J **39:** 886–893

Pandey SP, Roccaro M, Schön M, Logemann E, Somssich IE (2010) Transcriptional reprogramming regulated by WRKY18 and WRKY40 facilitates powdery mildew infection of *Arabidopsis*. Plant J **64:** 912–923

Pandey SP, Somssich IE (2009) The role of WRKY transcription factors in plant immunity. Plant Physiol **150:** 1648–1655

Park CJ, Ronald PC (2012) Cleavage and nuclear localization of the rice XA21 immune receptor. Nat Commun **3:** 920

Peng Y, Bartley LE, Canlas P, Ronald PC (2010) OsWRKY IIa transcription factors modulate rice innate immunity. Rice (N Y) **3:** 36–42

Peng Y, Bartley LE, Chen X, Dardick C, Chern M, Ruan R, Canlas PE, Ronald PC (2008) OsWRKY62 is a negative regulator of basal and *Xa21*-mediated defense against *Xanthomonas oryzae* pv. *oryzae* in rice. Mol Plant **1:** 446–458

Reddy AS, Marquez Y, Kalyna M, Barta A (2013) Complexity of the alternative splicing landscape in plants. Plant Cell **25:** 3657–3683

Rushton PJ, Somssich IE, Ringler P, Shen QJ (2010) WRKY transcription factors. Trends Plant Sci **15:** 247–258

Ryu HS, Han M, Lee SK, Cho JI, Ryoo N, Heu S, Lee YH, Bhoo SH, Wang GL, Hahn TR, et al (2006) A comprehensive expression analysis of the WRKY gene superfamily in rice plants during defense response. Plant Cell Rep **25:** 836–847

Seo PJ, Park MJ, Lim MH, Kim SG, Lee M, Baldwin IT, Park CM (2012) A self-regulatory circuit of CIRCADIAN CLOCK-ASSOCIATED1 underlies the circadian clock regulation of temperature responses in *Arabidopsis*. Plant Cell **24:** 2427–2442

Shen QH, Saijo Y, Mauch S, Biskup C, Bieri S, Keller B, Seki H, Ulker B, Somssich IE, Schulze-Lefert P (2007) Nuclear activity of MLA immune receptors links isolate-specific and basal disease-resistance responses. Science **315:** 1098–1103

Shimono M, Sugano S, Nakayama A, Jiang CJ, Ono K, Toki S, Takatsuji H (2007) Rice WRKY45 plays a crucial role in benzothiadiazole-inducible blast resistance. Plant Cell **19:** 2064–2076

Staiger D, Brown JW (2013) Alternative splicing at the intersection of biological timing, development, and stress responses. Plant Cell **25:** 3640–3656

Thordal-Christensen H, Zhang Z, Wei Y, Collinge DB (1997) Subcellular localization of H_2O_2 in plants: H_2O_2 accumulation in papillae and hypersensitive response during the barley-powdery mildew interaction. Plant J **11:** 1187–1194

Ueno Y, Yoshida R, Kishi-Kaboshi M, Matsushita A, Jiang CJ, Goto S, Takahashi A, Hirochika H, Takatsuji H (2013) MAP kinases phosphorylate rice WRKY45. Plant Signal Behav **8:** e24510

VanEtten HD, Mansfield JW, Bailey JA, Farmer EE (1994) Two classes of plant antibiotics: phytoalexins versus "phytoanticipins." Plant Cell **6:** 1191–1192

Walter M, Chaban C, Schütze K, Batistic O, Weckermann K, Näke C, Blazevic D, Grefen C, Schumacher K, Oecking C, et al (2004) Visualization of protein interactions in living plant cells using bimolecular fluorescence complementation. Plant J **40:** 428–438

Wang D, Amornsiripanitch N, Dong X (2006) A genomic approach to identify regulatory nodes in the transcriptional network of systemic acquired resistance in plants. PLoS Pathog **2:** e123

Wang H, Hao J, Chen X, Hao Z, Wang X, Lou Y, Peng Y, Guo Z (2007) Overexpression of rice *WRKY89* enhances ultraviolet B tolerance and disease resistance in rice plants. Plant Mol Biol **65:** 799–815

Whitham S, Dinesh-Kumar SP, Choi D, Hehl R, Corr C, Baker B (1994) The product of the tobacco mosaic virus resistance gene *N*: similarity to toll and the interleukin-1 receptor. Cell **78:** 1101–1115

Wu KL, Guo ZJ, Wang HH, Li J (2005) The WRKY family of transcription factors in rice and *Arabidopsis* and their origins. DNA Res **12:** 9–26

Xu X, Chen C, Fan B, Chen Z (2006) Physical and functional interactions between pathogen-induced *Arabidopsis* WRKY18, WRKY40, and WRKY60 transcription factors. Plant Cell **18:** 1310–1326

Yang S, Tang F, Zhu H (2014) Alternative splicing in plant immunity. Int J Mol Sci **15:** 10424–10445

Yokotani N, Sato Y, Tanabe S, Chujo T, Shimizu T, Okada K, Yamane H, Shimono M, Sugano S, Takatsuji H, et al (2013) WRKY76 is a rice transcriptional repressor playing opposite roles in blast disease resistance and cold stress tolerance. J Exp Bot **64:** 5085–5097

Yu D, Chen C, Chen Z (2001) Evidence for an important role of WRKY DNA binding proteins in the regulation of *NPR1* gene expression. Plant Cell **13:** 1527–1540

Yuan B, Shen X, Li X, Xu C, Wang S (2007) Mitogen-activated protein kinase OsMPK6 negatively regulates rice disease resistance to bacterial pathogens. Planta **226:** 953–960

Zipfel C, Robatzek S (2010) Pathogen-associated molecular pattern-triggered immunity: veni, vidi...? Plant Physiol **154:** 551–554